

Film cooling experimental investigation for ramped-conical holes geometry

Dr. Assim. H. Yousif, Dr. Kutaeba J. M. AL-Khishali, Falah F. Hatem

Abstract— The effect of introducing ramped-conical holes on film cooling performance has been investigated experimentally. Four models have been considered; model 1 consists of one row of cylindrical film cooling holes acting as the baseline case, model 2 consists of one row of single conical film cooling holes, model 3 consists of one row of single conical ramped-holes (upstream ramp with a backward-facing step), and model 4 consists of one row of double conical ramped-holes (upstream and downstream ramped-holes both with a backward-facing step). Detailed heat transfer coefficient and film effectiveness measurements are obtained simultaneously using a single test transient IR thermography technique. The study is performed at a single mainstream Reynolds number based on free-stream velocity and film hole diameter of 13000 at three different coolant-to-mainstream blowing ratios of 0.5, 1.0, and 1.5. The results show that film effectiveness is greatly enhanced when using ramp due to improved two dimensional natures of the film and lateral spreading, the distribution of laterally average film cooling effectiveness along the x-axis show that the double ramped-holes model provides promising film cooling performance particularly at moderate and high blowing ratios

Index Terms— Film cooling, effectiveness, conical, ramp, Enhancement

◆

IJSER

1 Introduction

Film cooling is one of the methods used to protect surfaces exposed to high-temperature such as, that exist in gas turbines by injection of coolant fluid (at a lower temperature than that of the main flow) to flood the surfaces to be protected. Bathie [1] stated that the advanced gas-turbine stages are designed to operate at increasingly higher inlet temperatures to increase thermal efficiency and specific power. This increase is made possible by advances in materials such as super alloys and thermal-barrier coatings and by cooling technology such as internal, impingement cooling. The inlet temperatures can far exceed allowable material temperatures by using cooling. Film cooling involved injection of coolant from film holes to forms a thin thermal barrier layer to protect the blade surface from the hot gases flow. The objective of film cooling is to achieve low heat transfer from the surrounding hot mainstream to the turbine blades, and large effectiveness on the blade surface. In the recent years several studies have been focused on developing the holes shape to enhance film cooling effectiveness. Film cooling research on flat surface is common, flat surface models can be used to study the effects of individual parameters with relative ease and are less expensive. Studies have proved that the results obtained on simple flat surface models can be applied to real engine designs with slight corrections Han et al. [2].

2 Film cooling operating parameters

Many investigators studied the effects of design and operating parameters on film cooling at which the cooling jets injected from one or two rows of inclined cylindrical holes. The studied parameters include film-cooling hole inclination, length-to-diameter ratio, spacing between holes, turbulence and embedded vortices in the hot-gas flow. The vortex system generated when cold jet injected in the hot main stream was described in details by Haven et al. [3] and Hyams et al. [4]. They showed the important role played by vortices in the evolution of film-cooling jets. The effects of hole geometry on the vortices dynamics of hot-gas/film-cooling jet interactions were investigated by Haven et al. [3], Hyams et al. [4], Kim and Kim [5]. Bunker [6] provided a comprehensive review of the research on hole shape. Haven and Kurosaka [7] examined the effects of placing vanes inside film-cooling holes that produce vortices in the same sense as the anti-kidney vortices. Zaman and Foss [8] and Zaman [9] steadied the effects of tabs

placed at the film-cooling-hole exit were steadies. Ekkad et al. [10] showed that placing tabs on the upstream side of the film-cooling-hole exit can improve film-cooling effectiveness. Proposal was made by Shih et al. [11] to place a strut or obstruction within each film-cooling hole that do not necessarily generate appreciable vortices but can cause vortices inside film-cooling holes to be stretched and tilted in a way that would change the magnitude and direction of the vortices in the CRVs and the anti-kidney pair. Bunker [12] proposed creating a trench about a row of film cooling holes to modify the boundary-layer/cooling jet interactions. Holes embedded in trench were found quite useful in improving film-cooling effectiveness as investigated by Altoraïri [13].

3 PAST STUDIES OF RAMPED- HOLES

The vortex system generates when cold jet injected in the hot main stream was described in details by Haven et al. [3] and Kelso et al. [14]. They showed the important role played by vortices in the evolution of film-cooling jets. One pair, referred to as the counter-rotating vortex pair (CRVs), was found to lift the jet off the surface that it is intended to protect and to entrain hot gas underneath it. The other pair, referred to an anti-kidney pair, was shown to have a sense of rotation opposite to that of the CRVs, and so can counteract the undesirable effects of the CRVs in entraining hot gas. Thus, it is of interest to develop strategies to control the formation and strength of these vortices in a way that leads to more effective film cooling. There are many ways to alter the structure of these vortices. Since the vortices in the cooling jet originates from the flow in the film-cooling hole, the boundary layer upstream of the film cooling hole, and the boundary-layer/cooling jet interactions, most investigators have focused on the geometry of the film-cooling hole. The boundary layer upstream of the film cooling hole can be altered by using ramped-holes concept to increase the adiabatic effectiveness of film cooling from row of film cooling holes. Sangkwon and Shih [15] proposed a geometry modification upstream of the holes to approach boundary layer flow and its interaction with the film cooling jets; this was done by making the surface just upstream of the holes row into a ramp with a backward-facing step. They showed numerically that an upstream ramp with a backward-facing step can greatly increase surface adiabatic effectiveness. The laterally averaged adiabatic effectiveness with a

ramp can be two or more times higher than without the ramp by increasing upstream and lateral spreading of the coolant. Shuping et al [16] examined experimentally on a concept for enhancing the film cooling performance by placing an upstream ramp in front of a row of cylindrical film cooling holes. They tested the upstream ramp with different angles ($\gamma = 8.5^\circ, 15^\circ,$ and 24°) and blowing ratios of (0.3, 0.4, 0.6, 0.9, and 1.4). In general, a relatively large ramp angle with a high blowing ratio leads to more effective film protection. Since extended surfaces such as a ramp could increase surface heat transfer and this is undesirable on the hot-gas side, it is noted that the ramp can be constructed in the thermal-barrier coating (TBC) system by using the ceramic top coat, which has very low thermal conductivity.

4 EXPERIMENTAL SETUP AND PROCEDURE

The experimental facilities consist of a low speed hot air supplier system with attached cold jet in the test section, as shown in Fig.1. The settling chamber of the test rig contains series rows of electrical heaters, row of honeycomb, and screens to ensure adequate hot air of uniform velocity and temperature throughout the test rig. The hot air routed through a convergent-divergent contraction having a rectangular cross-section before flowing through the test section. The bottom wall of the test section considered as testing plat, four plate models are considered, each model made of (234x123mm) Perspex plate of 0.8cm thickness. Fig.2 shows ramped-holes configurations with double ramped-holes arrangement. In order to allow the air to reach the desired temperature, the air is initially routed out away from the test section by using a by-bass gate passage. The temperature of the air is continuously monitored at the exit of the gate and when the desired temperature is reached, the gate is gradually fully opened.

Centrifugal air blower was used to supply the coolant air to the plenum. The plenum is located below the test model as shown in Fig.3. The coolant air enters a plenum then injected through holes into the test section. The coolant air pressure was measured at the inlet of the test section. Digital calibrated thermometers are used to measure the mainstream and coolant air temperatures. Pre-testing shows that all holes injected constant desired flow rate and temperature. The mainstream hot air temperature adjusted with a laboratory temperature (ambient air drawn by a blower) to give highest limit of ($T_c/T_h=0.4$). There are four models to be tested

each model having one row of five holes, considered here; model 1 consists of one row of cylindrical film cooling holes, model 2 consists of one row of conical film cooling holes without upstream ramp, model 3 consists of one row of conical film cooling holes with upstream ramp of backward-facing step, and model 4 consists of one row of conical film cooling holes with upstream and downstream ramps both of backward-facing step. Fig.3 shows the frontal views of models 3 and 4 configurations.

5 SURFACE TEMPERATURES MEASUREMENTS

The infrared thermograph system (Fluke Ti32) is used to measure surface temperatures. The thermal image can be displayed using standard color palettes or Ultra Contrast TM color palettes. The IR system is greatly affected by both background temperature and local emissivity. The test surface was sprayed with mat black color to increase the emissivity as a perfect black body. The temperature measurement taken is not accurately recorded unless the IR system is calibrated. The system is calibrated by measuring the temperature of the test surface using thermocouple type K and the reading of IR camera. The test surface is heated by mainstream hot air. The measured of temperatures obtained by both ways and they are recorded and stored during the heating process until achieving a steady state condition. Due to the emissivity of the test surface the temperature is obtained by IR camera is different from the temperature obtained by the thermocouple; therefore IR camera reading is adjusted until both temperatures reading are matched. The system calibration of the temperature range in present work is taken between -10°C and $+80^\circ\text{C}$. The test surface was modeled as a semi-infinite solid medium imposed by a sudden transient heating. The entire solid medium was initially at a uniform temperature before the transient test. During the transient heating test, each point on the surface will respond with different temperature at different time due to different heat transfer coefficient. The test surface is modeled as undergoing 1-D transient conduction with convective boundary conditions at the wall. Fig. (4) shows a schematic diagram of flow over a flat plate.

The test plate is initially at a uniform temperature, (T_i), and the convective boundary condition is suddenly applied on the plate at time, $t > 0$, (the hot stream of air provides a heat flux to the surface of

the plate and convective heat transfer phenomena occurs). The 2-D transient conduction equation is given by:

$$\frac{\partial^2 T}{\partial x^2} + \frac{\partial^2 T}{\partial y^2} = \frac{1}{\alpha} \frac{\partial T}{\partial t} \quad (1)$$

Neglecting the lateral conduction equation (1)

becomes:

$$\frac{\partial^2 T}{\partial x^2} = \frac{1}{\alpha} \frac{\partial T}{\partial t} \quad (2)$$

Solving equation (1) need two boundary conditions and an initial condition:

$$\text{Initial condition at } t = 0, T = T_i \quad (3)$$

$$\text{At } x = 0 \text{ and } t \geq 0 \quad -K \frac{\partial T}{\partial x} = h(T_w - T_m) \quad (4)$$

$$\text{At } x = \infty \text{ and } t \geq 0, T = T_i \quad (5)$$

The main approximation often applied to analyze transient conduction shown in Fig. (4) is the semi-infinite approximation. Semi-infinite solids can be visualized as very thick walls with one side exposed to some fluid, the other side remains unaffected by the fluid temperature since the wall is very thick. Solving the partial equation (1) with the prescribed initial condition and boundary conditions at $x = 0$ gives the transient response of the test plate wall due to the convective heat load applied by the hot mainstream air. The solution is given by the flowing equation [17].

$$\frac{T_w - T_i}{T_m - T_i} = 1 - \exp\left[\frac{h^2 \alpha t}{k^2}\right] \operatorname{erfc}\left[\frac{h\sqrt{\alpha t}}{k}\right] \quad (6)$$

Where h is the unknown quantity in the equation with T_w is the wall temperature at time t after the initiation of the transient test. The material properties, α ($1.0752 \times 10^{-7} \text{ m}^2/\text{s}$) and k (0.1873 W/m.K) [17] dictate the applicability of the semi-infinite solid solution.

The assumptions of semi-infinite solid are valid for this work because the transient test duration is small, usually less than 60 seconds and also because of the test surface is made of Perspex which has low thermal conductivity, low thermal diffusivity and low lateral conduction, combinations of the above facts make sure that heat is conducted only in the x -direction and it does not reach the bottom of the test surface.

In film cooling case, the film should be treated as a mixture of air mainstream and the coolant air. The mainstream temperature (T_m) in equation (6) has

to be replaced by the film temperature (T_f). Equation (6) has two unknowns (h and T_f). To solve this equation, two sets of data points are required to obtain the unknowns. In this case, a transient infrared thermograph technique will be used to obtain both h and η from a single test as described by Ekkad et al. [18]. Thus, two images with surface temperature distributions are captured at two different times during the transient test.

The IR images for models test surface at each test are captured and stored by the memory of the thermal camera. These images are transferred to PC. The IR images are converted to corresponding temperature digital values and then saved as data in Excel sheet. MATLAB programs Software are prepared by using a semi-infinite solid assumption to introduce the film cooling effectiveness and heat transfer coefficient contours.

6 Film cooling effectiveness

A non-dimensional temperature term is known as the film cooling effectiveness (η), and is defined as:

$$\eta = \frac{T_f - T_m}{T_c - T_m} \quad (7)$$

The term blowing ratio (BR) is used to study the effect of the amount of coolant flow to mainstream flow. It is defined as the ratio of the mass flux of the coolant to the mass flux of the mainstream ($BR = \rho_c U_c / \rho_m U_m$).

The verification of the current experimental approach, the test results of the baseline case (model 1) is made by comparison with the experimental results of the similar case study of baseline case of Yuen [19]. Sample of results at $BR = 1$ of adiabatic spanwise averaged film cooling effectiveness distribution along the X/D together with that of Yuen [19] experimental results are presented in Fig.(6). The results show approximately similar levels of (η) with slightly different in local values. It is fair to say that the results obtained from the present experiments are in good agreement with experimental results of Yuen [19].

Experimental results of the present investigation are in the thermal aspect in the form of distribution and contour plots of various variables including the film cooling effectiveness and heat transfer coefficient.

The ramped-holes models geometry are design from holes inclined at $\theta = 35^\circ$, the hole spacing between adjacent holes was $3.5D$, in both ramped-holes models, the configurations are taken as ramps (length = $2.5D$ and $\gamma=16.7^\circ$) located at a distance ($\beta=0$) from the hole edge.

Fig.7 shows the comparison of spanwise averaged film cooling effectiveness distribution along the normalized streamwise distance (X/D). The present average value covers one pitch distance of $-1.75 < Z/D < 1.75$. Both ramped-holes cases (models 3 and 4) show rapid decaying particularly with increasing downstream distance from the hole. For blowing ratios of 0.5 & 1 the ramped-hole case provided better cooling effectiveness than (model 1 and 2). At $BR=1.5$ double ramped-holes provide highest and significant improvement in the laterally averaged film cooling effectiveness. In general better performance at moderate and high blowing ratios ($BR = 1.0$ and 1.5) is contributed by the existing of double ramps. The double ramps contribute to lesser penetration of coolant jet into mainstream allowing the coolant air to remain close to the wall compared with the three other cases. Also from this figure it can be seen that for single ramp case (Model 3), the adiabatic film cooling effectiveness is enhanced in the lateral area at $BR=1$ and this is confirmed by the film cooling effectiveness contours presented in Fig.8.

The overall area averaged film cooling effectiveness ($\bar{\eta}$) for single ramped-holes (model 3) is enhanced by (134%, 292.6%, and 554.6%) at ($BR=0.5, 1.0,$ and 1.5) respectively. All enhancements are calculated with reference to the conventional single cylindrical holes row (model 1). Results of double ramped-holes case (model 4) show that the overall area averaged film cooling effectiveness is enhanced greatly by (130.3%, 343.7%, and 679.4%) at ($BR=0.5, 1.0,$ and 1.5) respectively. In general, the results clearly show the benefits of adding double ramps to the conventional single conical holes row, in which there is almost a 679.4% increase in overall area averaged film cooling effectiveness at $BR = 1.5$.

7 Heat load

In the practical application, turbine designers are concerned with the reduction of heat load to the film protected surface. The heat load can be simulated by combining the film cooling effectiveness (η) and heat transfer coefficient ratio (h/h_o), therefore the ratio (q/q_o) can be introduced to present the reduction in heat flux at the test

surface with the presence of coolant air. A net heat flux ratio is used to measure the combined effect of film effectiveness and heat transfer coefficient. The following relation between (η) and q/q_o as given by Ekkad and Zapata [20] may be used to estimate (q/q_o):

$$\frac{q}{q_o} = \frac{h}{h_o} \left(1 - \frac{\eta}{\phi} \right) \quad (8)$$

The verification of the current calculation method of spanwise averaged heat transfer coefficient ratio (\bar{h}/h_o) is made by comparison with the experimental results of Lu [21] for the baseline case (model 1). Sample of comparison results of (\bar{h}/h_o) at $BR=1$ along the normalized streamwise distance (X/D) are presented in Fig.9, both results are in good agreement.

Fig.10 presents detailed spanwise averaged heat transfer coefficient ratio (\bar{h}/h_o) at $BR=1$. The heat transfer coefficient ratio for ramps cases is increased compared to the baseline case. Such increase are due to the interaction between the coolant jet and the mainstream flow, this interaction produced high turbulence region. Several studies have shown that jet injection produces increased turbulence level inside the boundary layers due to the shear layer mixing and this is the main reason that (h) downstream of hole show higher values according to Nasir et al. [22]. At present test at the downstream region ($X/D > 10$) the heat transfer coefficients have higher values and remain in the same level up to the end of the test surface. It is clear in the ramped-holes case, the heat transfer coefficient increased over that of (models 1 and 2).

Heat flux ratio indicates the reduction in heat flux on the test surface from the film injection. As indicated by Akkad and Zapata [20], if the value of the net heat flux ratio is less than 1.0, then the introduction of film cooling has beneficial effect. If the value is greater than 1.0, it can be said that the film cooling did not serve its purpose of cooling.

Fig.11 represents the effect of (BRs) on overall area-averaged heat flux ratio (\bar{q}/q_o). All models show good results of (\bar{q}/q_o) except for (model 1 and) at blowing ratio of 1.5 the values of (\bar{q}/q_o) is exceed unity.

8 CONCLUSION

Double ramped- conical holes are recently proposed to improve the two dimensional natures and lateral spreading of the film cooling. Film

cooling effectiveness, heat transfer coefficients, and heat flux ratio were evaluated by using semi-infinite solid assumption with the aid of the measurements of model surface temperatures by transient infrared thermography technique. The film cooling performance was found to be enhanced greatly by introducing single and double ramped holes compared to baseline (conventional single jet holes row). Accepted performance is obtained at moderate and high blowing ratios for double ramped-holes. The ramped-holes increase film effectiveness over that of the baseline by (554.6%) for single ramped-holes and by (679.4%) for double ramped-holes at BR=1.5. The heat transfer coefficient ratio increased as compared to the baseline case, this is due to the interaction between the jet and the main stream which produces a region of high turbulence.

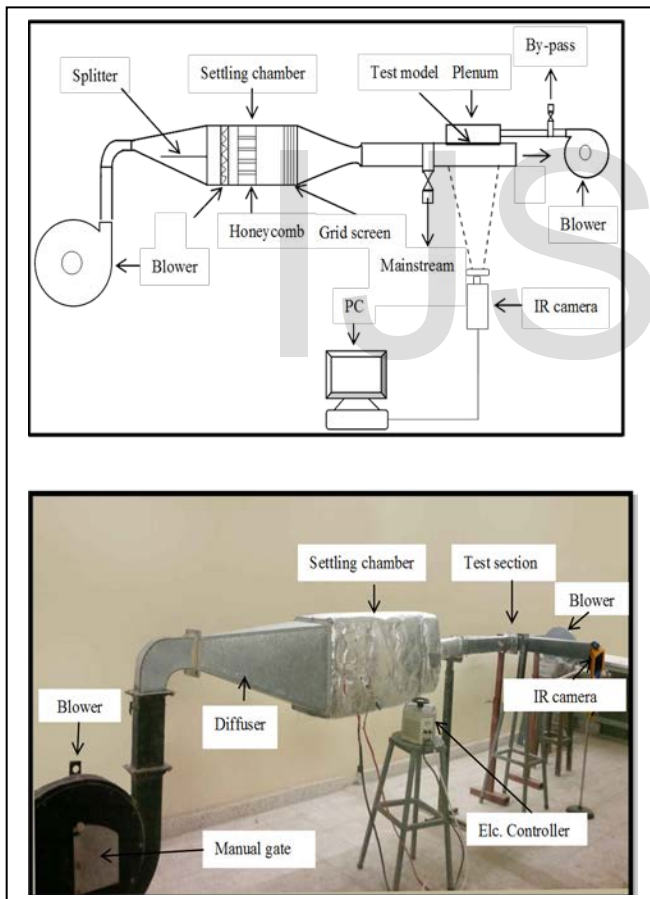
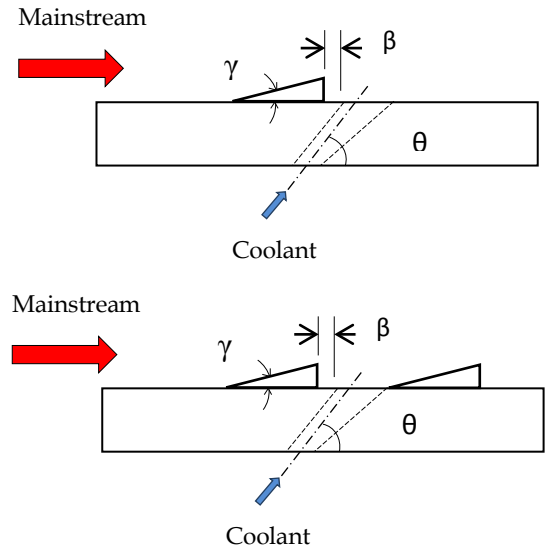


Figure (1) Photography and schematic of the experimental test rig

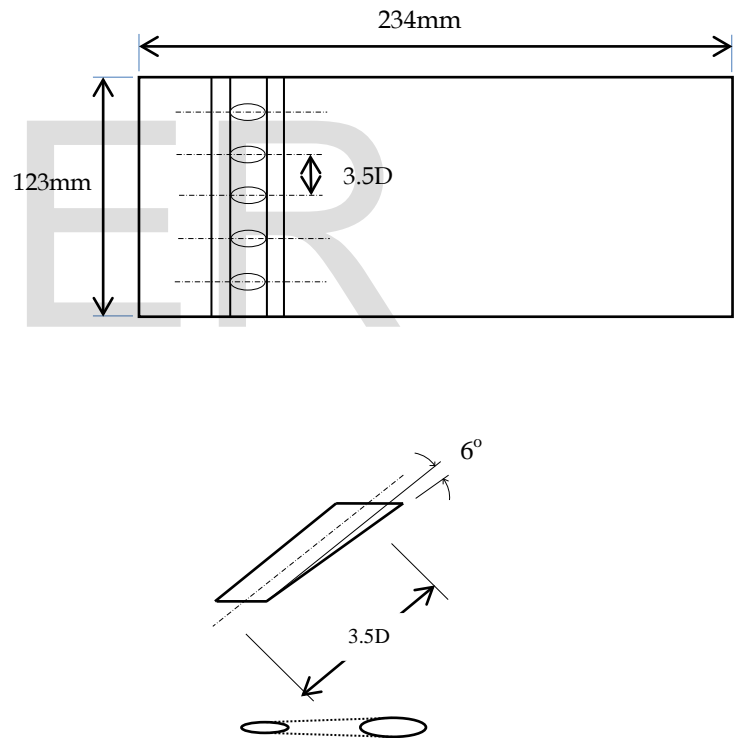


Figure (2) Schematic of ramped-holes configurations

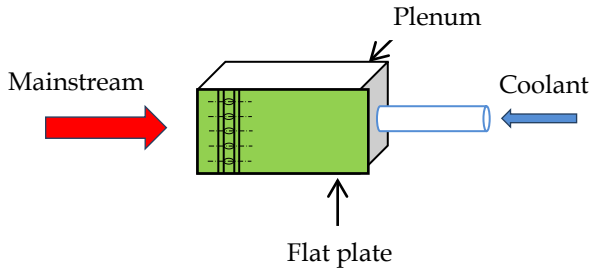


Figure (3) Schematic of test section

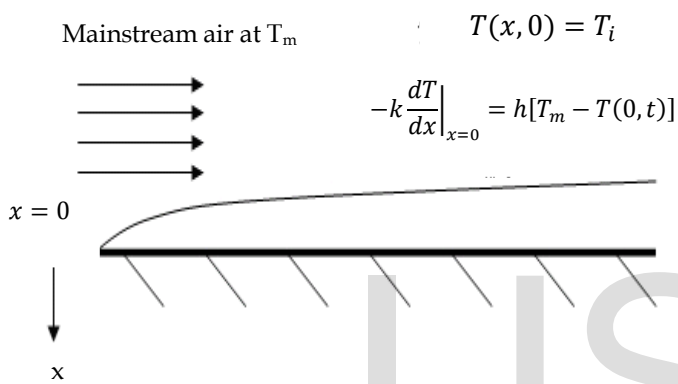


Figure (4) Flow over a flat plate

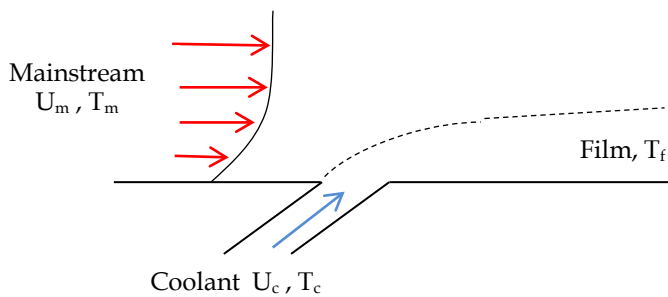


Figure (5) Film cooling over a flat plate

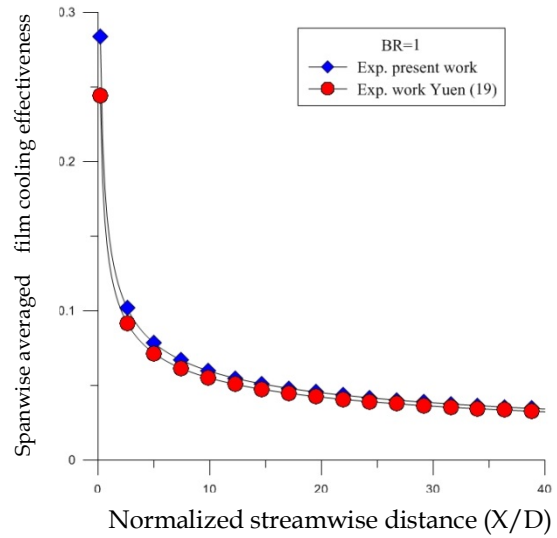
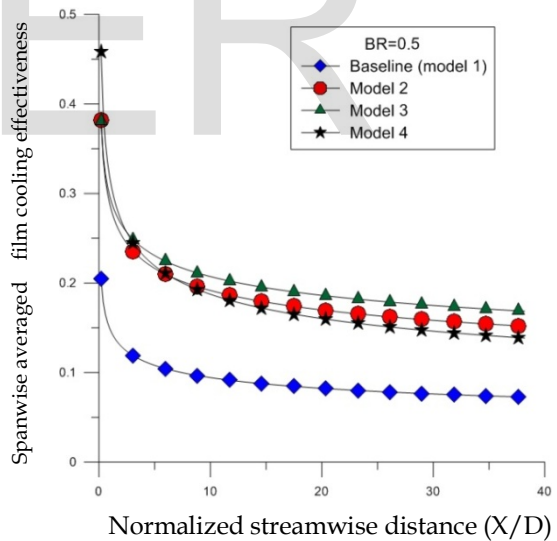


Figure (6) Verification of the present study with the experimental results of Yuen [19]



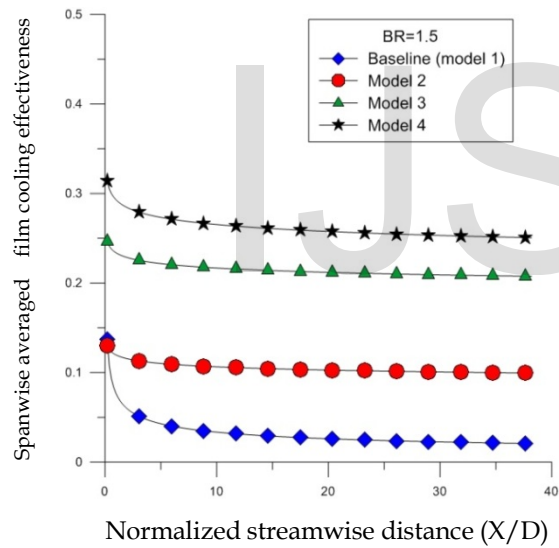
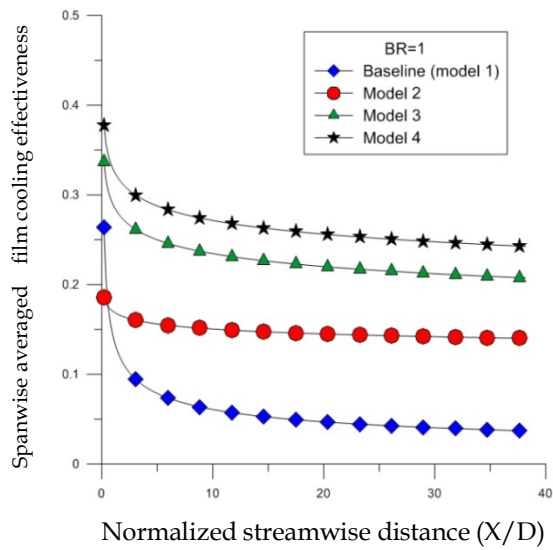


Figure (7) Comparison of spanwise averaged film cooling effectiveness ($\bar{\eta}$) distribution along the normalized streamwise distance (X/D) for different models at different BRs.

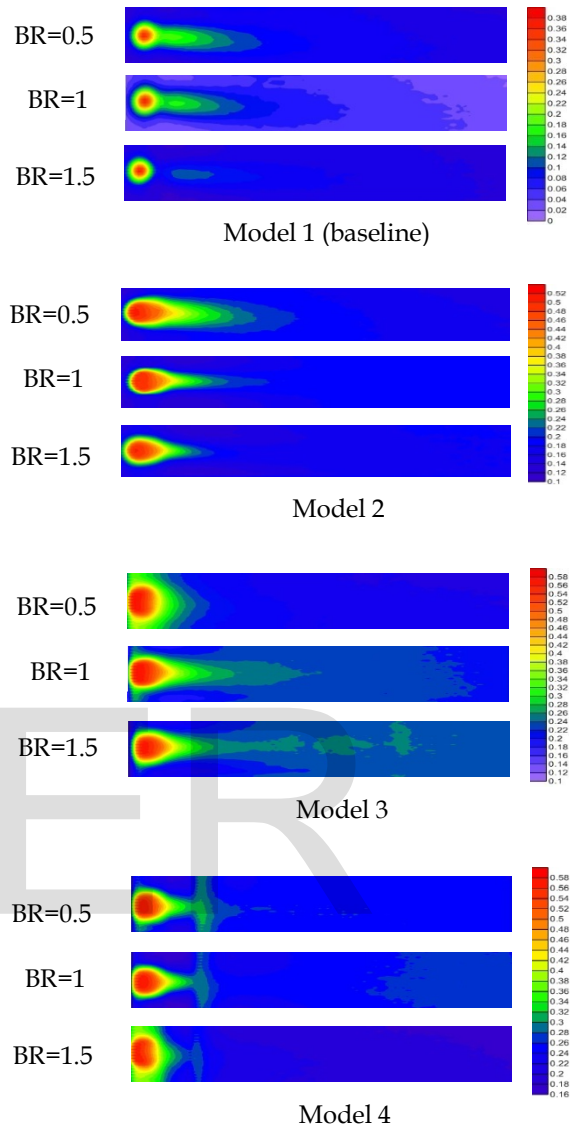


Figure (8) Film cooling effectiveness contours for different models

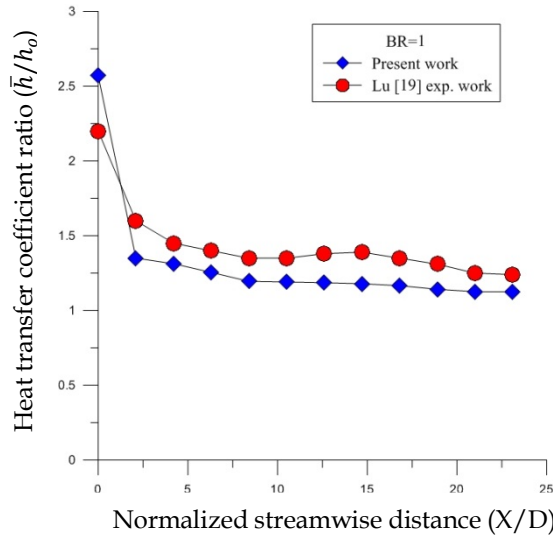


Figure (9) Verification of experimental results of heat transfer coefficient ratio (\bar{h}/h_o) of the present study with the experimental results of Lu [20]

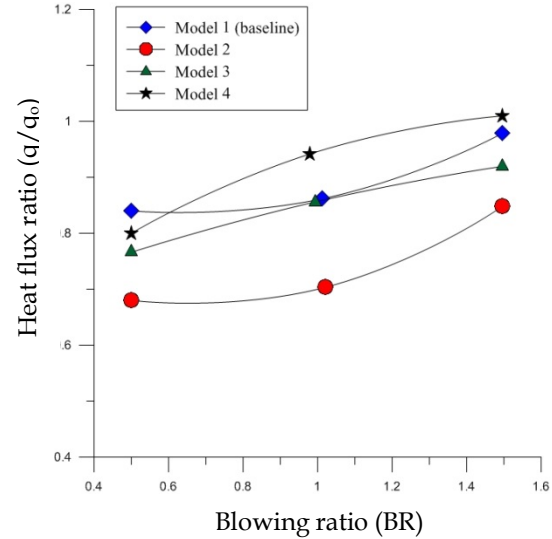


Figure (11) Effect of blowing ratio on overall area-averaged heat flux ratio for conical hole cases

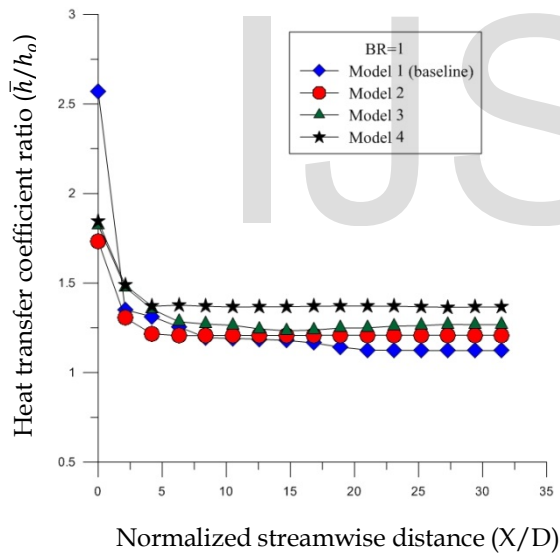


Figure (10) Effect of hole configuration on spanwise averaged heat transfer coefficient ratio for different models

REFERENCES

- [1] W. W. Bathie, Fundamentals of gas turbines. Second edition, John Wiley & Sons, Inc (1996).
- [2] J. C. Han, H. Du, S.V. Ekkad. "Gas turbine heat transfer and cooling technology". Taylor & Francis Group (2001).
- [3] Haven, B.A., Yamagata, D.K., Kurosaka, M., Yamawaki, S., Maya, T., 1997, "Anti-kidney Pair of Vortices in Shaped Holes and their Influence on Film Cooling Effectiveness" ASME Paper 97-GT-45.
- [4] D. G. Hyams, K. T. McGovern, J. H. Leylek. Effects of geometry on slot-jet film cooling performance. ASME Paper No. 96-GT-187 (1997).
- [5] J. K. Kim, S. -M. Kim. Influence of shaped injection holes on turbine blade leading edge film cooling. Int. J. Heat and Mass Transfer 47 (2004) 245-256.
- [6] R. S. Bunker. A review of shaped hole turbine cooling technology. ASME J. Heat Transfer, 127 (2005) 441-453.
- [7] B. A. Haven, M. Kurosaka, Improved jet coverage through vortex cancellation. AIAA J., 34(11) (1996) 2443-2444.
- [8] K. B. M. Q. Zaman, J. K. Foss. The effects of vortex generators on a jet in a cross-flow. Phys. Fluids, 9(1), (1997) 106-114.
- [9] K. B. M. Q. Zaman. Reduction of a jet penetration in a cross-flow by using tabs. AIAA Paper No. 98-3276 (1998).

- [10] S. V. Ekkad, H. Nasir, S Acharya. Flat surface film cooling from cylindrical holes with discrete tabs. *J. Thermophys. Heat Transfer* 17(3) (2003) 304-312.
- [11], T. I.-P. Shih, Y.-L. Lin, M. K. Chyu, S. Gogineni, Computations film cooling from holes with struts. ASME paper No. 99-GT-282 (1999).
- [12], R. S. Bunker. Film cooling effectiveness due to discrete holes within transverse surface slots. Proceedings IGTI Turbo Expo, Amsterdam, the Netherlands, ASME Paper No. GT-2002-30178 (2002).
- [13] M. S. Altorairi. Film cooling from cylindrical holes in transverse slots, MSc. thesis, Louisiana State University (2003), Baton Rouge, LA, USA.
- [14] R. M. Kelso, T. T. Lim, A. E. Perry. An experimental study of round jets in cross-flow. *J. Fluid Mech.* 306(1996) 111-144.
- [15] Na. Sangkwon, T. I.-P. Shih. Increasing adiabatic film-cooling effectiveness by using an upstream ramp. *Journal of Heat Transfer* Vol.129 (2007) 464-470.
- [16] S. P. Chen, M. K. Chyu, T. I.-P. Shih, Effects of upstream ramp on the performance of film cooling, Int. J. Thermal Sciences Vol. 50, Issue 6 (June 2011) 1085-1094.
- [17] F.P. Incropera, D. Dewitt. *Fundamentals of heat transfer*, Wiley & Sons, New York, NY . (2006),.
- [18] Ekkad, S. V., Ou, S. and Rivir, R. V., 2004, "A Transient Infrared Thermography Method for Simultaneous Film Cooling Effectiveness and Heat Transfer Coefficient Measurements from a Single test," GT2004-54236, Proceedings of ASME Turbo Expo 2004, Vienna, Austria.
- [19] Yuen, C. H.N. and Botas, R.F.M., 2003, "Film cooling characteristics of a single round hole at various stream wise angles in a cross flow: Part I effectiveness", *International Journal of Heat and Mass Transfer*, Vol. 46, PP. 221-235.
- [20] S.V. Ekkad, D. Zapata. Heat transfer coefficients over a flat surface with air and CO₂ injection through compound angle holes using a transient liquid crystal image method. *ASME J. Turbomachinery* 119 No. 3 (1997) 580-586.
- [21] Lu, Y., Dhungel, A., Ekkad, S.V., and Bunker, R.S., 2007, "Effect of Trench Width and Depth on Film Cooling from Cylindrical Holes Embedded in Trenches", ASME Paper GT 2007-27388.
- [22] H. Nasir, S. Acharya, S. Ekkad. Improved film cooling from cylindrical angled holes with triangular tabs: effect of tab orientations. *Int. J. Heat and Fluid Flow* 24 (2003) 657-668.